

Receiving and transmitting light-like radio waves: Antenna effect in arrays of aligned carbon nanotubes

Y. Wang^{a)} and K. Kempa

Boston College, Chestnut Hill, Massachusetts 02467

B. Kimball and J. B. Carlson

US Army, Natick Soldier Center, Natick, Massachusetts 01760

G. Benham

Mega Wave Corporation, Boylston, Massachusetts 01505

W. Z. Li

Florida International University, Miami, Florida 33199

T. Kempa, J. Rybczynski, A. Herczynski, and Z. F. Ren

Boston College, Chestnut Hill, Massachusetts 02467

(Received 4 June 2004; accepted 26 July 2004)

We present optical measurements of random arrays of aligned carbon nanotubes, and show that the response is consistent with conventional radio antenna theory. We first demonstrate the *polarization effect*, the suppression of the reflected signal when the electric field of the incoming radiation is polarized perpendicular to the nanotube axis. Next, we observe the interference colors of the reflected light from an array, and show that they result from the *length matching* antenna effect. This antenna effect could be used in a variety of optoelectronic devices, including THz and IR detectors. © 2004 American Institute of Physics. [DOI: 10.1063/1.1797559]

In recent years, periodic and random arrays of multi-walled carbon nanotubes (MWCNTs) have been synthesized on various substrates, by the plasma-enhanced chemical vapor deposition (PECVD) process.^{1–4} Each nanotube in such arrays is a metallic rod of about 50 nm in diameter and 200–1000 nm in length.⁵ Therefore, one can view interaction of these arrays with the electromagnetic radiation as that of an array of dipole antennas.^{6,7} Since the most efficient antenna interaction occurs when the length of the antennas is of the order of the wavelength of the incoming radiation, we expect an antenna-like interaction of MWCNT arrays with visible light. There are two major antenna effects. First, the polarization effect suppresses the response of an antenna when the electric field of the incoming radiation is polarized perpendicular to the dipole antenna axis. Second, the antenna length effect maximizes the antenna response when the antenna length is a multiple of half-wavelength of the radiation.⁷ The polarization antenna effect has already been observed in the Raman response of single-walled carbon nanotubes.⁸ The nanoscopic dipole antenna length effect was recently observed in microbolometer, stripline antennas.⁹ In this letter, we demonstrate both of these antenna effects in random MWCNT arrays. We choose in this study random nanotube arrays to suppress the intertube diffraction, which obscures the intratube antenna effects that are of interest here.

Our MWCNT arrays are fabricated using PECVD. The Si substrate is coated with a thin film of Ni catalyst (20 nm) in a dc magnetron sputtering system, that is then heated to 550–600 °C in a PECVD reaction chamber to break up the Ni film into small catalyst particles. A gas mixture of NH₃ and C₂H₂ is introduced into the PECVD chamber at the ratio of 2:1, and a dc glow discharge plasma is then generated and

maintained by a bias voltage of 500–550 V. A growth time of about 1–2 min yields nanotubes around or shorter than 1000 nm. Figure 1(a) shows the scanning electron microscope (SEM) image of such an array of random MWCNTs. By modifying the growth parameters, and/or the geometry of the bias voltage electrodes, a nonuniform growth of nanotubes, with average length varying across the sample, can also be achieved. This has been utilized to produce the samples used in the present study.

We first demonstrate the polarization effect. We coated the surface of a small piece of a Si wafer (2 × 1 cm²) with a thin film of Cr. Subsequently, one-half of the sample was coated with a thin film of Ni catalyst, and processed to grow a random array of MWCNTs. The sample was illuminated with white unpolarized light, and observed in a specular direction through a rotating polarizer. Figure 2 (left inset) shows that when the polarizer is oriented parallel to the growth direction of the nanotubes (orientation angle $\Theta=0^\circ$), the light reflected from the array is clearly visible, while the exposed metallic half of the sample is dark (not reflecting). With increasing (or decreasing) angle Θ , intensity of the light reflected from the nanotube array diminishes, while the intensity reflected from the metallic side increases until at

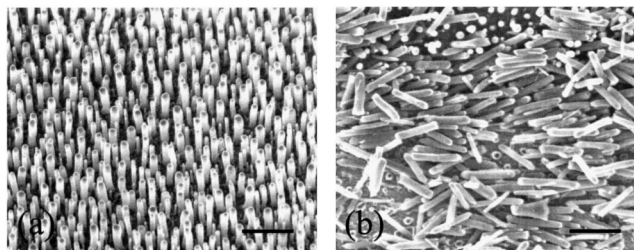


FIG. 1. Aligned (a) and scratched (b) random arrays of MWCNTs. In this study we use only the random arrays, to reduce the internanotube diffraction effects. Scale bars, 1 μm .

^{a)} Author to whom correspondence should be addressed; electronic mail: wanyq@bc.edu

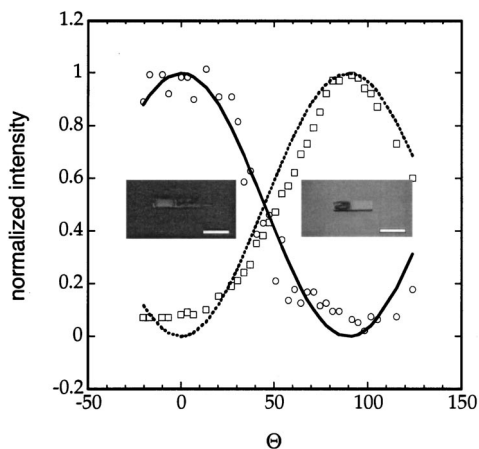


FIG. 2. Polarization effect. Reflected, normalized light intensity vs polarization angle Θ for the sample shown in the insets. Circles represent the light intensity from the random array of nanotubes, and squares from the metallic film. Lines represent the expected functional dependencies: $I = \cos^2\theta$ for nanotubes (solid), $I = \sin^2\theta$ for metallic film (dotted). Left inset: sample viewed with the polarization plane parallel to nanotubes (p -polarization), $\Theta = 0^\circ$. Right inset: sample viewed through polarizer with the polarization plane perpendicular to nanotubes (s -polarization), $\Theta = 90^\circ$. Scale bars, 1 cm.

$\Theta = 90^\circ$, the radiation is observable essentially only from the metallic side (see Fig. 2, right inset).

This behavior follows from the fact that, while in nanotubes currents are excited predominantly along their length, in the metallic film, currents flow in the film plane; that is, perpendicular to the nanotubes. Each nanotube acts as an antenna reradiating light with the electric field E , polarized in the plane parallel to the antenna. A polarizer, with its axis of polarization rotated by an angle Θ to this plane, transmits radiation with a projected electric field $E' = E \cos \theta$, and therefore the corresponding observed intensity is given by the familiar law of Malus $I_{NT} \propto (E')^2 = E^2 \cos^2 \theta$ (solid line-circles in Fig. 2). For light reflected from the metallic film the situation is exactly “out-of-phase” with that for the array; that is, $I_{metal} \propto (E'')^2 = E^2 \sin^2 \theta$ (dotted line-squares in Fig. 2).

The second characteristic effect of an antenna is its resonant response behavior as a function of the radiation wavelength. This results from the condition that the induced current oscillations must “fit” into the antenna length (i.e., satisfy the boundary conditions at the antenna ends). A general equation describing the scattering maxima from a random array of dipole antennas (with vanishing current at each end) is

$$L = m \frac{\lambda}{2} f(\theta, n), \tag{1}$$

where $f(\theta, n) = 1$ for a single, simple dipole,^{7,10} and $f(\theta, n) = (n^2 - \sin^2 \theta)^{-1/2}$ in the limit of the very dense array (thin film limit),¹¹ where the average interantenna distance $D \ll \lambda$. For $D \sim \lambda$, or $D \gg \lambda$, $f(\theta, \lambda) \approx 1$, and is only weakly dependent on the angle θ . We expect similar behavior for the random array of MWCNTs.

Figure 3(a) shows a sample of a random array of nanotubes with gradually reduced lengths (from left to right) illuminated by white light. The strong interference colors are due to the antenna length effect. Figure 3(b) shows the intensity of the reflected light at the specular direction versus the radiation wavelength of the incoming radiation measured at selected spots (positions $A_1 - A_7$) of the sample shown in Fig. 3(a). Experiments were done using the Ocean Optics

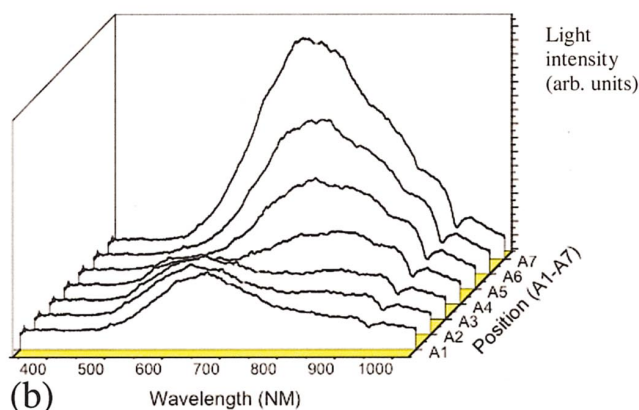
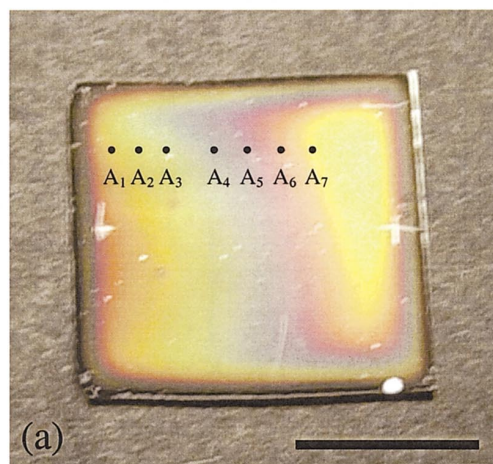


FIG. 3. (Color) Antenna length effect. (a) Interference colors from the random array of MWCNTs. $A_1 - A_7$ are the selected positions where the length and optical measurements were carried out. Scale bar, 1 cm. (b) Reflected light intensity vs radiation wavelength measured in selected points on the sample shown in (a).

USB2000 Fiber Optic Spectrometer (FOS). White light emerging from a 50- μ m-diameter fiber was focused onto the sample surface at 30° angle of incidence. Incident spot size was of the order of 0.5 mm. A receiving fiber with a 1 mm diameter is positioned to collect light reflected spectrally from the sample surface. The system was first corrected for dark field and then normalized with respect to the tungsten light source and reflectance from the silicon substrate at the 30° incident angle. Another sample, with longer nanotubes, produced insufficient scattered light intensity for the FOS, and the wavelength was estimated using a high sensitivity CCD camera and optical filters, with accuracy of about 10%. The exact positions at which the data were acquired were permanently marked (scratched with a needle) on each of the samples. The SEM pictures were then used to estimate the average nanotube length at each marked spot. To minimize the parallax error of this estimate, we measured only the collapsed (lying flat on the surface) nanotubes in the scratched area, as shown in Fig. 1(b).

In addition to the experiments, we have performed computer simulations of the electromagnetic response from a random dipole antenna array.¹² We model the array as a set of 10 parallel, equal-length antennas, randomly distributed on, and perpendicular to, a flat substrate. Antenna dimensions and the average interantenna distance represent the ac-

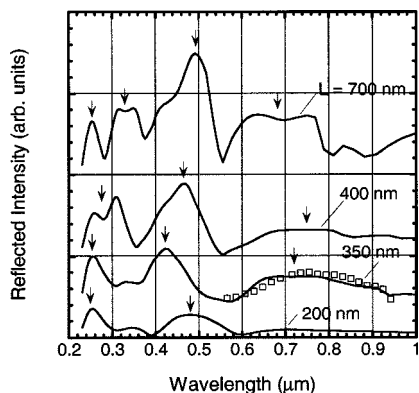


FIG. 4. Calculated reflected light intensity spectra for a model array of random antennas, for various nanotube lengths. Squares represent an experimental result [Fig. 3(b), for position A_5] shown for comparison.

tual nanotube array. The dielectric constant of the substrate is assumed to be real and equal to 10. The resulting reflection curves, for various antenna lengths are shown in Fig. 4.

Figure 5 combines the experimental and theoretical results to demonstrate the antenna length effect. In this figure, positions of the various reflected intensity maxima are plotted versus the corresponding average antenna length L . Solid lines represent the ideal dipole antenna condition [Eq. (1), with $f=1$] for different m . The measured results are represented as solid circles and squares. Crosses mark positions of the distinct maxima of the theoretical curves. Arrows indicate those maxima in Fig. 4. It is clear that both experimental and theoretical results follow closely the ideal dipole antenna condition, and thus demonstrate that MWCNTs, as expected, can act as light antennas.

We can also estimate the quality of the nanotube antennas. Figure 4 shows a comparison between one of the experimental curves of Fig. 3(b) (for position A_5) shown as squares, and the corresponding calculated response. This comparison shows that the calculation, which assumed infinite conductivity of the metallic antenna, reproduces well the measured line width of the peak. Therefore, the peak width is primarily due to the radiation losses and inhomogeneous broadening, and not to the resistive losses of currents induced inside the nanotubes. From this we conclude that the actual scattering rate of the conducting electrons (γ) in the nanotube antenna must be much less than the width of the

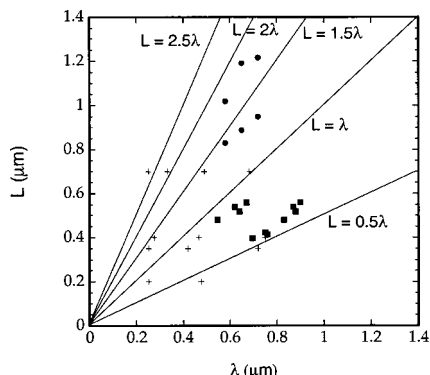


FIG. 5. Antenna length effect. Average length of MWCNTs vs wavelength of the incoming radiation at the corresponding maxima of reflected light intensity. From sample evaluated using FOS (filled squares), and CCD camera (filled circles). Solid lines represent the simple dipole antenna condition [Eq. (1)]. Crosses mark maxima of the calculated reflected light intensity spectra, shown in Fig. 4.

peak in Fig. 4. After replotting the peak versus frequency (rather than the wavelength), we find that the width is about 10^{15} s^{-1} , and therefore γ must be of the order of 10^{14} s^{-1} or less. This is a very low scattering rate, of the order of (or better than) that for good metals such as copper.¹³

The fact that MWCNTs act as high quality light antennas, suggests various applications based on the radio analogy. For example, a THz demodulator could be build, if a sufficiently fast diode is attached to (or built into) each antenna in the array mounted on a THz stripline. The modulating THz signal could then be seamlessly introduced into the stripline by shining modulated light onto the array. This scheme could be used in a new generation of THz and possibly IR detectors. The antenna length effect can be tuned by controlling the nanotube length, and to some extent the array density during the growth process, making the devices frequency selective. In principle, the antenna effects should be also detectable in, and the same applications possible with, arrays of aligned single-walled nanotubes. However, at this moment no scheme for making such arrays of all metallic single-walled nanotubes exists, and there is no reason to believe that such systems would have any advantage over those based on MWCNTs.

In conclusion, we have demonstrated that MWCNTs interact with light in the same manner as simple dipole radio antennas. In particular, they show both the polarization and the length antenna effect. The first effect is characterized by a suppression of the reflected signal when the electric field of the incoming radiation is polarized perpendicular to the nanotube axis. The second, the antenna length effect, maximizes the response when the antenna length is a proper multiple of the half-wavelength of the radiation. These effects could be used in a variety of optoelectronic devices, such as THz or and IR detectors.

This work is supported partly by The US Army Natick Soldier Systems Center under the grant DAAD16-02-C-0037, and partly by NSF under the grant NIRT 0304506. Donation of MWCNT samples by NanoLab, Inc., is also acknowledged.

¹Z. F. Ren, Z. P. Huang, J. W. Xu, J. H. Wang, P. Bush, M. P. Siegal, and P. N. Provencio, *Science* **282**, 1105 (1998).
²K. B. K. Teo, M. Chhowalla, G. A. J. Amaratunga, W. I. Milne, D. G. Hasko, G. Pirio, P. Legagnenx, F. Wyczisk, and D. Pribat, *Appl. Phys. Lett.* **79**, 1534 (2001).
³L. Delzeit, C. V. Nguyen, R. M. Stevens, J. Han, and M. Meyyappan, *Nanotechnology* **13**, 280 (2002).
⁴Z. P. Huang, D. L. Carnahan, J. Rybczynski, M. Giersig, M. Sennett, D. Z. Wang, J. G. Wen, K. Kempa, and Z. F. Ren, *Appl. Phys. Lett.* **82**, 460 (2003).
⁵K. Kempa, B. Kimball, J. Rybczynski, Z. P. Huang, P. F. Wu, D. Steeves, M. Sennett, M. Giersig, D. V. G. L. N. Rao, D. L. Carnahan, D. Z. Wang, J. Y. Lao, W. Z. Li, and Z. F. Ren, *Nano Lett.* **3**, 13 (2003).
⁶R. J. Crowley, U. S. Patent No. 6,258,401 (10 July 1997).
⁷F. E. Terman, *Electrical and electronic engineering series*, 3rd ed. (McGraw-Hill, New York, 1947), Chap. 14, pp. 662–668.
⁸A. Jorio, A. G. Souza Filho, V. W. Brar, A. K. Swan, M. S. Ünlü, B. B. Goldberg, A. Righi, J. H. Hafner, C. M. Lieber, R. Saito, G. Dresselhaus, and M. S. Dresselhaus, *Phys. Rev. B* **65**, 121402R (2002).
⁹C. Fumeaux, M. A. Gritz, I. Codreanu, W. L. Schaich, F. J. Gonzalez, and G. D. Boreman, *Infrared Phys. Technol.* **41**, 271 (2000).
¹⁰P. Moon and D. E. Spencer, *Field theory for engineers* (Van Nostrand, Princeton, NJ, 1961).
¹¹O. S. Heavens, *Optical Properties of Thin Films* (Dover, New York, 1965).
¹²These calculations use the Numerical Electromagnetics Code, NEC-4.1D, authored by G. Burke *et al.*, Lawrence Livermore National Laboratory.
¹³G. Burns, *Solid State Physics* (Academic, Orlando, 1985).